

# Development of a novel bunch oscillation recorder with RFSoc technology

---

R. Nomaru,<sup>1</sup> G. Mitsuka,<sup>2</sup> L. Ruckman,<sup>3</sup> and R. Herbst<sup>3</sup>

<sup>1</sup>*The University of Tokyo, Bunkyo, Tokyo 113-0033, Japan*

<sup>2</sup>*KEK, Oho, Tsukuba, Ibaraki 305-0801, Japan*

<sup>3</sup>*SLAC National Accelerator Laboratory, 2575 Sand Hill Road, M/S 96, Menlo Park, CA 94025, USA*

*E-mail:* [nomaru@g.ecc.u-tokyo.ac.jp](mailto:nomaru@g.ecc.u-tokyo.ac.jp)

## ABSTRACT:

The SuperKEKB accelerator is designed to achieve unprecedented luminosity levels, but this goal is currently hindered by Sudden Beam Loss (SBL) events. These events not only obstruct luminosity improvement but also pose a significant risk to accelerator components, the Belle II detectors, and the superconducting focusing system, potentially leading to severe damage and quenching of the superconducting system. To address this critical challenge, we have developed a novel Bunch Oscillation Recorder (BOR) based on RFSoc technology. The BOR has demonstrated high precision with a position resolution of 0.03 mm, making it a powerful tool for real-time beam monitoring. In its initial deployment, the BOR successfully recorded multiple SBL events, providing valuable data for further analysis. By strategically positioning BORs at the suspected points of SBL origin, we aim to directly identify sources of beam instability. We anticipate that this portable, high-speed BOR monitor will play a crucial role in resolving the SBL issue, ultimately helping achieve SuperKEKB's luminosity targets.

**KEYWORDS:** Beam diagnostics; RFSoc; Particle accelerator; Instrumentation

---

## Contents

<b>1</b>	<b>Background and Motivation</b>	<b>1</b>
<b>2</b>	<b>Hardware</b>	<b>3</b>
2.1	Overview	3
2.2	Vacuum chamber and button electrode	3
2.3	Analog circuit	4
2.4	ZCU111 evaluation board	5
2.5	Calculation of bunch position	7
<b>3</b>	<b>Firmware</b>	<b>7</b>
<b>4</b>	<b>Software</b>	<b>9</b>
<b>5</b>	<b>Testing</b>	<b>9</b>
5.1	Overview	9
5.2	Test using a local beam bump	10
5.3	Test using the feedback system	10
<b>6</b>	<b>Observation of Sudden Beam Loss</b>	<b>12</b>
<b>7</b>	<b>Summary</b>	<b>14</b>
<b>8</b>	<b>Acknowledgements</b>	<b>14</b>

---

## 1 Background and Motivation

The SuperKEKB accelerator [1] collides electrons and positrons at very high luminosity, providing large quantities of  $B$  mesons,  $\tau$  leptons, and other charged particles for the Belle II detector. The accelerator consists of a 7 GeV electron storage ring (HER) and a 4 GeV positron storage ring (LER). By adopting a nanobeam scheme, the beam size at the collision point was narrowed down to a nanometer level, and the world's highest luminosity record,  $4.7 \times 10^{34} \text{ cm}^{-2} \text{ s}^{-1}$ , was achieved in 2022. The accelerator resumed operations in February 2024 after its first long shutdown (LS1) of over a year. We are operating towards even higher luminosity, but a phenomenon called Sudden Beam Loss (SBL) is hindering luminosity improvement [2].

The SBL event is presently the biggest obstacle to increasing luminosity at SuperKEKB. SBL events have caused cracks in accelerator components such as collimators, damage to the Belle II detector, and quenches in the superconducting focusing system. Figure 1 shows how the SBL events have damaged a tantalum-made collimator head [3]. Note that 31 collimators in both rings protect the Belle II detector from unwanted beam losses. Collimator head replacement involves removing

damaged and scattered head material (tungsten or tantalum) from the vacuum pipe and restoring the pressure in the vacuum pipe to the ultra-high vacuum level after it has deteriorated to the atmosphere level during the replacement process. Therefore, the entire replacement process usually takes several days to a week. We find, even empirically, that the higher the stored bunch current than 0.7 mA/bunch, the more frequently SBL events occur, followed by severe damage. Thus, we hesitate to increase the stored beam current as anticipated, hindering the increase in instantaneous luminosity. In addition, once the SBL events occur, leading to beam aborts or the superconducting system quenching, recovery to regular beam operation takes several hours or a day. Therefore, since SBL events limit the both accumulation of integral luminosity and increase instantaneous luminosity, they have become a critical issue in SuperKEKB operations. Nevertheless, the cause of the SBL event and the location of its occurrence have yet to be identified.

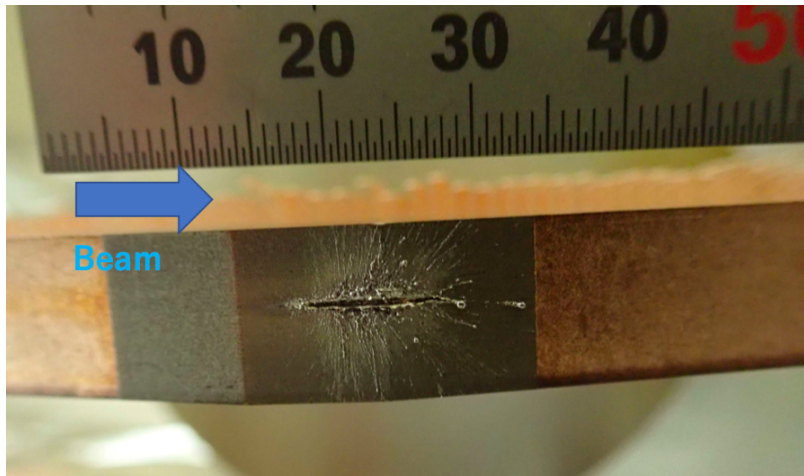


**Figure 1.** Damaged collimator head due to the sudden beam loss event in LER.

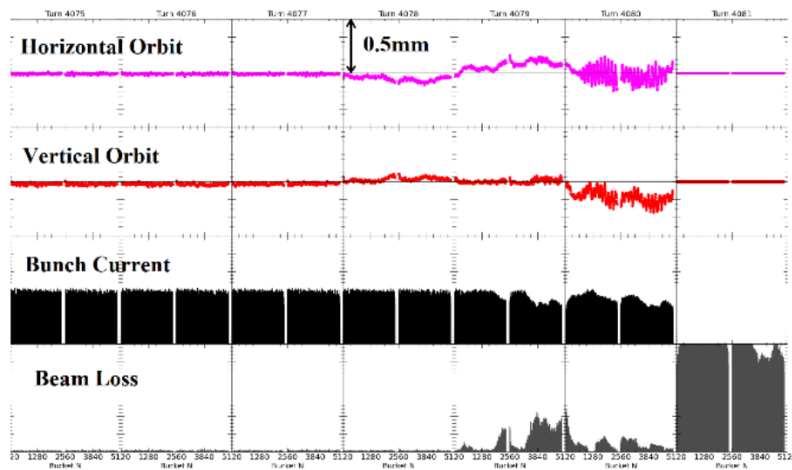


**Figure 2.** Example of the sudden beam loss event. Bunch-by-bunch horizontal orbit, vertical orbit, bunch current, and bunch current loss from the top.

A Bunch Oscillation Recorder (BOR) is a beam instrument that records the beam position

bunch-by-bunch for ten or more turns before a beam abort occurs. Before LS1, one VME-board-type BOR, 18K10 by Digitex Co., Ltd, hereafter we call it VME-BOR, was equipped for each ring [4]. VME-BORs in each ring have been placed in the Fuji straight section in the SuperKEKB main ring and taken bunch-by-bunch oscillation data for more than 4000 turns before every beam aborts. With the measurements with the VME-BORs, we found that when SBL occurred, it accompanied a sizable bunch position oscillation. Figure 2 [5] demonstrated that the horizontal and vertical bunch orbit moved firstly, about three turns before the beam abort, followed by the beam loss of  $\sim 10\%$ . The vertical division indicates one turn. Such observation indicates that some unknown sources, potentially residual dust, beam instabilities, and an imperfect feedback kicker system kick a portion of bunches, leading to bunch position oscillation and significant beam loss. However, only one VME-BOR in each ring cannot pinpoint where and how SBL events initially occur. It cannot distinguish two possible scenarios: small kick amplitude and degeneracy in the betatron phase advance. Thus, we realize the necessity of placing multiple BORs to cover phase advances widely and more directly detect the bunch oscillation near suspicious incidence locations. The VME-BOR design is over ten years old, and the many parts used inside the circuit, such as the 8-bit ADC, are unavailable today. In light of this situation, our aim in the project is to develop a "handy" BOR ready for post-LS1 operation and place several copies of it along the ring.

## 2 Hardware

### 2.1 Overview

The new BOR was developed using a novel integrated chip solution referred to as an RF System on Chip (RFSoc), which was developed by AMD. The RFSoc has been acknowledged as a significant advancement in the fields of radio frequency and digital signal processing. Data converters and programmable logic are integrated into a single package by the RFSoc, designed to streamline the development of high-performance radio frequency systems [6, 7]. This R&D effort was undertaken using the ZCU111 RFSoc evaluation board [8]. Signals from the button electrodes in the accelerator vacuum chamber are input to RFSoc, sampled, and compared to measure the position of bunches. Figure 3 shows the schematic diagram of the RFSoc-based BOR system we developed.

### 2.2 Vacuum chamber and button electrode

Figure 4 shows the design of the vacuum chamber used for this R&D. This is a bunch-by-bunch orbit feedback BPM (FB-BPM) chamber [9], installed in the Fuji straight section of the SuperKEKB accelerator. This Low Energy Ring (LER) chamber is equipped with button electrodes primarily for the SuperKEKB feedback system, but there are some unused electrodes, which we used. Of the button electrodes arranged in a cross pattern, two electrodes facing each other in the vertical direction were used. The diameter of the chamber in the area where the button electrode is installed is 64 mm. Figure 5 (Left) shows a picture of this FB-BPM chamber. In the center of it, several cables are attached, which are connected to the button electrodes in the beam pipe. Figure 5 (Right) shows a photograph of the button electrode attached to the FB-BPM chamber. It has a diameter of 6 mm, is sealed with glass, and features an SMA connector [9, 10].

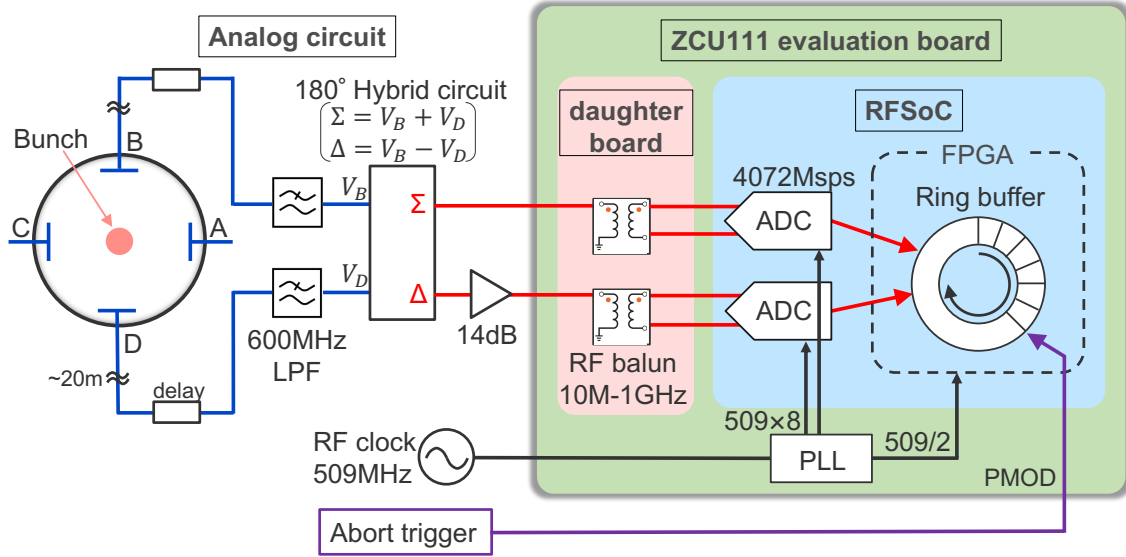


Figure 3. Schematic diagram of the RFSoc-based BOR system

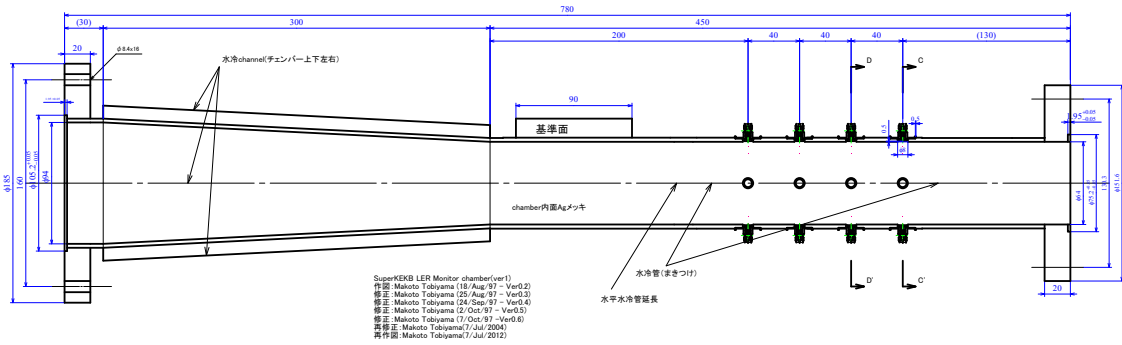
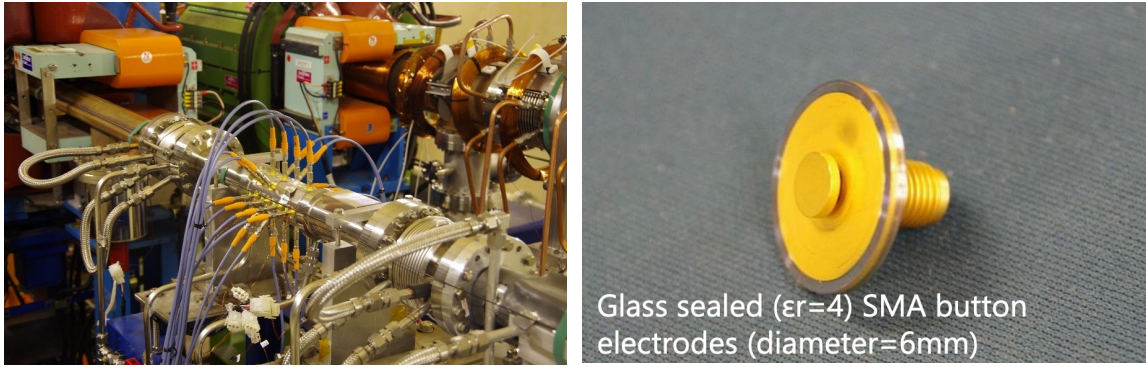


Figure 4. Design of the SuperKEKB FB-BPM chamber

### 2.3 Analog circuit

The variable-length coaxial tube made by Nihon Koshuha Co., Ltd. [11] is connected to the button electrodes with an approximately 20 m cable. All circuits after this coaxial tube are located in a room without radiation, isolated from the tunnel where the accelerator is located. This variable-length coaxial tube is a delay circuit with adjustable length and is used to align the timing of signals from the two button electrodes.

After this, the 600 MHz low-pass filter (LPF) is used to remove high-frequency noise from the signal. We use LPF because the cutoff frequency of a typical vacuum chamber in SuperKEKB LER is 990 MHz [1]. The cutoff frequency of the FB-BPM chamber we are using here is higher than 990 MHz, but we use the 600 MHz LPF to create a BOR that can be used in various places in the SuperKEKB ring. This LPF is the 5LP8-600B-SR made by LORCH [12]. We chose this LPF because, after testing various types of LPFs by inputting signals from button electrodes, we found that this LPF by LORCH produced an output waveform with the least ringing and tails and



**Figure 5.** (Left) The SuperKEKB FB-BPM chamber. The cable visible in the center of the photo is connected to the button electrode inside the beam pipe. (Right) The button electrode attached to the FB-BPM chamber. This has a diameter of 6 mm, is sealed with glass, and has an SMA connector.

would not affect the successive bunch signal arriving at an interval of 4 ns minimum. The frequency response of this filter is shown in Figure 6. This is the  $S_{21}$  parameter of this LPF measured with the network analyzer E5071C made by Keysight Technologies [13]. The bandwidth of this network analyzer is from 300 kHz to 20 GHz. From Figure 6, we can see that  $S_{21}$  is about -3 dB at 600 MHz, which confirms that this is functioning properly as an LPF with a cutoff frequency of 600 MHz.

The outputs of the LPF are then fed into a 180-degree hybrid circuit to extract the sum signal " $\Sigma$ " and the difference signal " $\Delta$ ". The hybrid circuit is the H-183-4-SMA, made by MACOM [14]. In the 100-1500 MHz range, the insertion loss of this hybrid circuit is 1.5 dB maximum, the isolation is 20 dB minimum, and the VSWR is 1.6:1 maximum. Figure 7 (left) shows the output signals of the hybrid circuit measured by an oscilloscope. The yellow waveform is  $\Sigma$ , and the green waveform is  $\Delta$ . The oscilloscope is RTO2024, made by Rohde & Schwarz, with a sampling speed of 10 GSps and a bandwidth of 2 GHz [15]. The signals shown in Figure 7 (left) are from the button electrode attached to the FB-BPM chamber of the LER. This shows the signal from one bunch with a bunch current of about 1 mA and this waveform was recorded on February 8, 2024. The bunch spacing is 6 ns or more.

Since the  $\Delta$  signal is small, it is passed through an amplifier after the hybrid circuit. We are using the THS4303EVM amplifier evaluation board made by Texas Instruments [16]. THS4303 amplifier chip [17] is implemented on this evaluation board, and it is a fixed-gain and single-ended amplifier. It has an amplification factor of 20 dB and a bandwidth of 1.8 GHz. In this evaluation board, an amplification of 14 dB is achieved by impedance matching at 50  $\Omega$ . At the typical bunch current of 1 mA, the  $\Delta$  signal is around 50 mV high, so amplifying it by 14 dB increases it to around 250 mV, which is within the input range of the RFSoc's ADC, 1 V peak-to-peak. Additionally, this evaluation board has single-ended SMA ports for both analog inputs and analog outputs, which are compatible with the output port of the hybrid circuit and the analog input port of the ZCU111 evaluation board after that.  $\Sigma$  and  $\Delta$  signals are then input into the ZCU111 evaluation board.

## 2.4 ZCU111 evaluation board

The ZCU111 evaluation board utilizes a first-generation RFSoc that supports eight channels of 12-bit ADCs (up to 4.096 Gsps) and eight channels of 14-bit DACs (up to 6.554 Gsps). Synchro-

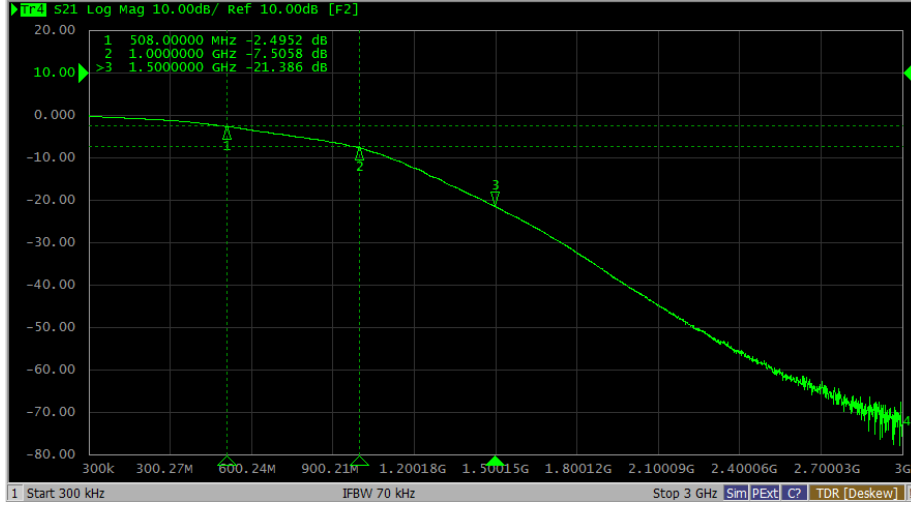


**Figure 6.** Frequency response of low-pass filter 5LP8-600B-SR by LORCH. This is the  $S_{21}$  parameter of this low-pass filter measured with a network analyzer.



**Figure 7.** (Left) Hybrid circuit output measured by an oscilloscope. The yellow waveform is  $\Sigma$  and the green waveform is  $\Delta$ . This shows the signal from one bunch in the LER with a bunch current of about 1 mA. (Right) The digital signal recorded by the RFSoc with the sampling frequency of 4.072 Gsps. The orange waveform is  $\Sigma$  and the green waveform is  $\Delta$ . This shows the signal from one bunch in the LER with a bunch current of about 0.2 mA.

nization of the ADCs' sampling frequency and the FPGA clock frequency inside RFSoc with the SuperKEKB RF clock 509 MHz [1] is achieved through an external clock input and phase locked loops (PLLs). The ZCU111's ADC inputs and DAC outputs are connected to SMA connectors via an AMD daughter card called XM500 RFMC (Radio Frequency Mezzanine Card) [18]. Four of the eight ADC inputs are designated for differential signals, while the other four accept single-ended signals. Two of the single-ended channels are connected to a TCM2-33WX+ balun made by Mini-Circuits [19] for 10 MHz to 1 GHz ("Low Frequency"), and the remaining two channels are connected to a BD1631J50100AHF balun made by Anaren [20] for 1 to 4 GHz ("High Frequency").

In our usual cases, we used "Low Frequency" (LF) baluns on the XM500 daughter board. Through the LF balun, the signal is input into the RFSoc and is digitized by the RF-ADC. Digital signals are sent to the FPGA. The FPGA is equipped with ring buffers that temporarily holds these

digital signals. Figure 7 (Right) shows the signal from the button electrode attached to the FB-BPM chamber of the LER, passed through the analog circuit described in Section 2.3, and measured by the RFSoc with the sampling frequency of 4.072 Gsps. The orange waveform is  $\Sigma$  and the green waveform is  $\Delta$ . This shows the digital signal from one bunch with a bunch current of about 0.2 mA and this was recorded on February 16th, 2024. The bunch spacing before and after this bunch is 8 ns or more. The sampling frequency of 4.072 Gsps is made with the 8-fold multiplication of the SuperKEKB RF frequency 509 MHz. The sampling frequency and phase are correctly synchronized with the SuperKEKB RF frequency to keep lock the sampling point to the peak of the bipolar signal of successive bunches. By acquiring points at time intervals that are multiples of the RF period, it is possible to measure positions of all bunches that come at intervals of 4 ns minimum.

The abort kicker trigger signal of SuperKEKB is received via the ZCU111's PMOD (Peripheral Module) GPIO (General Purpose Input/Output) interface. This abort kicker trigger is issued when the loss monitors installed throughout the accelerator observe radiation exceeding a certain threshold value and this activates the abort kicker, causing the beam to be aborted. When this GPIO receives this signal, it issues a fault trigger to a ring buffer. In the current firmware design, the ring buffer saves digital signals for 101 turns before the abort. This enables bunch-by-bunch measurement of beam instability for about 1 ms just before the beam abort. This is because one turn takes about 10  $\mu$ s so 101 turns correspond to about 1 ms.

## 2.5 Calculation of bunch position

We can obtain the bunch positions using the ratio of two voltage signals from the button electrodes facing each other. Here, we assume the vertical position  $y$ . We calculate  $y$  by using the voltages of the electrodes facing each other ( $V_B$  and  $V_D$  in Figure 3) with

$$y = k_y \frac{V_B - V_D}{V_B + V_D} = k_y \frac{\Delta}{\Sigma} \quad (2.1)$$

where  $k_y$  is a constant calculated by the boundary element method and  $\Delta = V_B - V_D$ ,  $\Sigma = V_B + V_D$ . The FB-BPM chamber has electrodes arranged in a cross pattern, so the position can be determined using the voltages of only two electrodes facing each other.

When calculating the position based on the digital signals recorded by the RFSoc, we take the peak of the bipolar signal for each  $\Sigma$  and  $\Delta$  (red points in Figure 7 (Right)), compute their ratio and multiply by  $k_y$  during offline analysis.

## 3 Firmware

The firmware running on the RFSoc is illustrated in a block diagram in Figure 8. At the core of the digitization process, the Radio Frequency Data Converter (RFDC) block is positioned as a hardened IP within the RFSoc, responsible for the conversion of ADC and DAC data. Configured to operate at 4.072 GSPS across 4 channels, the ADC, capable of a maximum of 4.096 GSPS, receives analog signals. Similarly, the DAC, which has a maximum capability of 6.554 GSPS, is set to operate at 6.108 GSPS, converting digital data back into analog signals across 4 channels. Sourced from the SuperKEKB RF reference, a 509 MHz reference clock is utilized. The internal Phase Lock Loops

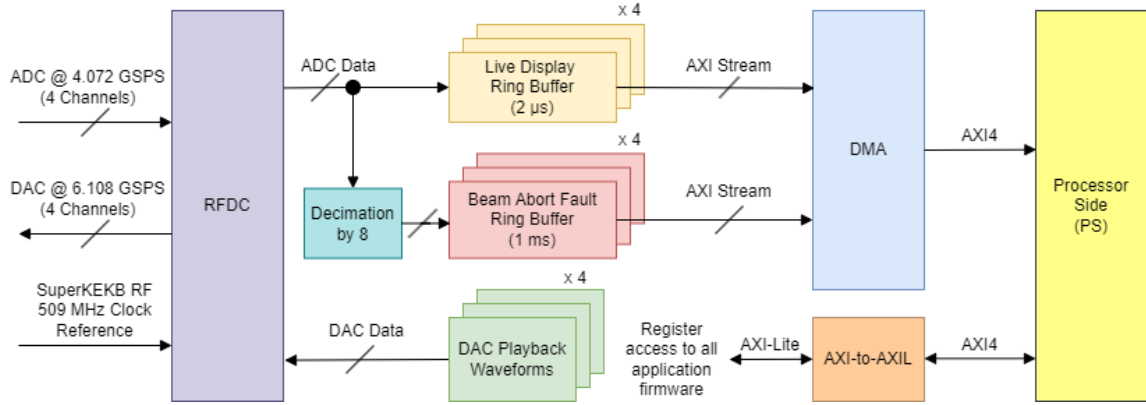


**Figure 8.** Block diagram of the firmware

(PLLs) of the RFDC convert this 509 MHz reference clock into a 4.072 GHz sampling clock for the ADC channels and a 6.108 GHz sampling clock for the DAC channels. At a higher integer multiple of the 509 MHz reference clock, the DAC channels are operated faster than the ADC channels to provide improved waveform generation.

Digital data from the ADC channels are stored in two types of ring buffers: live display and fault. The live display buffers, which have a depth of two microseconds, are triggered periodically and asynchronously by software to update the waveform display. This aids in monitoring and debugging. In contrast, the fault buffers, which have a depth of approximately 1 ms, are triggered by a beam abort signal connected to the ZCU111's PMOD interface. These fault buffers record the signal at a decimated rate of 8, a necessary reduction to maximize the buffer depth. Additionally, the firmware provides the capability to manually trigger the fault buffer from software for monitoring and debugging purposes unrelated to faults. The data from the readout ring buffer is transmitted as an AXI Stream to the Direct Memory Access (DMA) block using the AXI Stream protocol [21]. Subsequently, the DMA transfers the data over an AXI4 interface to the Processor Side (PS) using the AXI4 memory protocol [22].

The DAC channels are used to emulate the BPM signals for early firmware and software development when a BPM is not available for testing. The software can load waveform patterns into the Programmable Logic's (PL's) memory for each DAC channel, making them appear identical to a typical BPM signals. Next, the firmware plays back these loaded waveforms through the RFDC's digital DAC interface. This playback can be either continuous or occur for a programmable number of iterations. To use this BPM emulation, the DAC SMA connectors and ADC SMA connectors on the XM500 daughter card are connected together via coaxial cables. This emulation mode is only used in development and is not intended for actual BOR measurements on the beamline.

Control and register access to all application firmware components are managed via an AXI-Lite interface [22]. A protocol conversion from the PS's native AXI4 memory interface to an AXI-Lite interface is utilized.

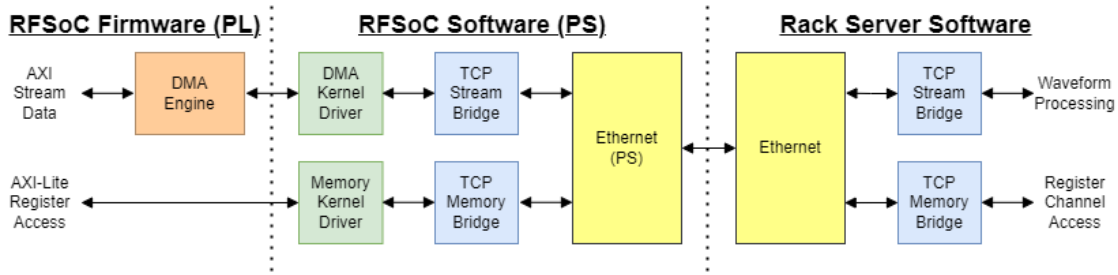


**Figure 9.** Block diagram of the software register access and waveform streaming.

## 4 Software

The software register access and waveform streaming processes are illustrated in the block diagram in Figure 9. This communication involves three main components: RFSoc firmware, RFSoc software, and rack server software. Within the RFSoc firmware, waveforms are transmitted to the DMA engine and DMA kernel driver via the AXI Stream interface, while AXI-Lite register access is directed to the memory kernel driver. The memory kernel driver restricts user access to registers outside the application firmware context. The TCP stream bridge converts the received waveforms into TCP messages for Ethernet communication. Similarly, the TCP memory bridge translates the register access request and response messages between the memory kernel driver and the Ethernet TCP interface. On the rack server side, complementary TCP stream and TCP memory bridges translate the TCP messages back into the native run control software interfaces. Petalinux (6.1.30-xilinx-v2023.2) is used on the RFSoc for the Linux kernel.

The run control software used in this testing, known as "Rogue," is designed for both rapid prototyping and experiment deployment. It can operate in either a Python/C++ hybrid mode or a C++-only mode, and is supported on x86-64, ARM32, and ARM64 architectures [23]. In this application, the Rogue software runs on both the RFSoc and rack server to utilize a common library for the TCP stream/memory bridge. The RFSoc's application register mapping within Rogue is defined using Python classes. The waveform receiver is also defined within a Python class, which converts the native byte array into a 16-bit numpy array for waveform data processing and analysis. Additionally, a GUI was developed on top of the Rogue software to assist in the live display of BPM waveforms and register diagnostics. Screenshots of this GUI are shown in Figure 10. The GUI software is based on the Python Display Manager (PyDM), a PyQt-based framework for building user interfaces for control systems [24].

## 5 Testing

### 5.1 Overview

We performed two types of tests on the RFSoc-based BOR using two button electrodes vertically attached to the FB-BPM chamber of the LER. The first test was to evaluate the accuracy of the position measurement using a local beam bump, and the second test was to check whether the RFSoc-based BOR is working properly as a bunch-by-bunch detector using SuperKEKB's feedback system.

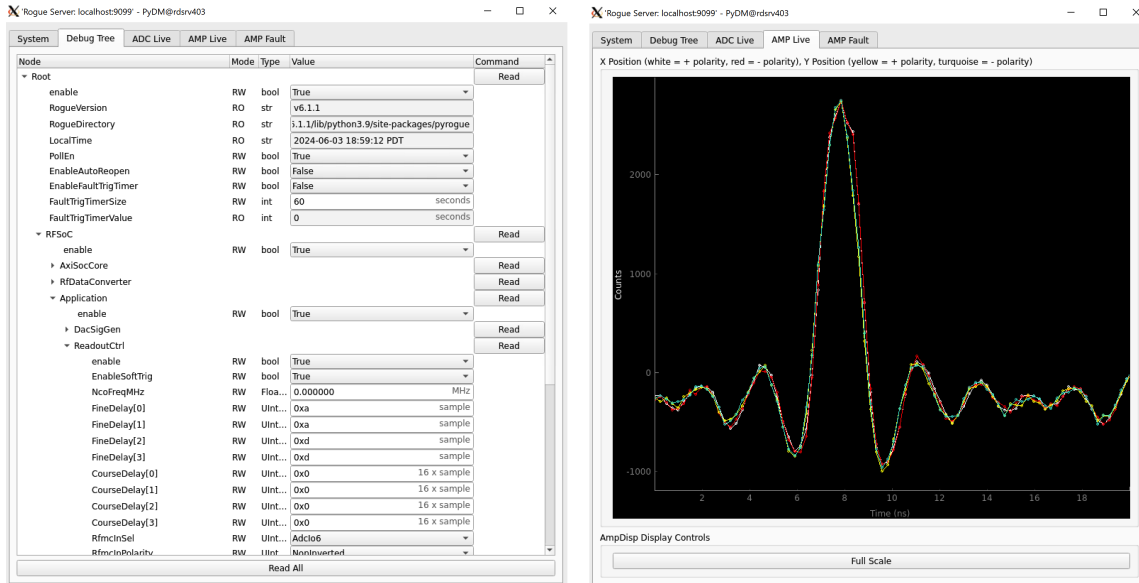


**Figure 10.** Screenshots of the software GUI running on the rack server. (Left) Debug Tree for peak/poke of the RFSoc’s registers, (Right) Live Display of the BPM waveforms.

## 5.2 Test using a local beam bump

To evaluate the position resolution, we performed a test using a local beam bump. We created a beam bump in the vertical direction with steering magnets surrounding the FB-BPM and measured the bump position using the RFSoc-based BOR. This test was carried out on February 23, 2024, using the LER beam. With 97 bunches, the spacing was wide enough that the tail of the signal did not affect other bunches. The bunch current was approximately 0.5 mA and the amplitude of the  $\Sigma$  signal was about 250 mV. The beam bump position was adjusted based on measurements from narrow-band detectors, with a resolution of about 4  $\mu\text{m}$  [1]. The results of this test are shown in Figure 11. We can see the calculated vertical positions from RFSoc-based BOR using the equation 2.1 (vertical axis of Figure 11) demonstrate good agreement with the bump positions (horizontal axis of Figure 11). The red line is a linear fit of the measured points, which confirms good linearity of the RFSoc-based BOR. The standard deviation at each measurement point is approximately 30  $\mu\text{m}$ . Since this value is much greater than the resolution of the narrow-band detector ( $\sim 4 \mu\text{m}$ ) used to set the bump position, we assume that the effect of the bump setting accuracy on the measurement results is negligible. The resolution of 30  $\mu\text{m}$  meets our target accuracy of 0.1 mm or less. Since it was known that bunch position oscillations of several hundred micrometers occur during the SBL, as shown in Figure 2, this target value was set as a condition for capturing the oscillation behavior of SBL.

## 5.3 Test using the feedback system

We validated the performance of the RFSoc-based BOR by comparing its position measurements with those from an established bunch-by-bunch detector. Specifically, we used the FB-BPM detector, which is the detector used in the bunch-by-bunch feedback system [25] located in the Fuji straight section. The feedback system uses the iGp12 made by Dimtel, inc. [26], which includes digitizers, FPGA which contains tap filters, etc. This feedback system has been operated at SuperKEKB,

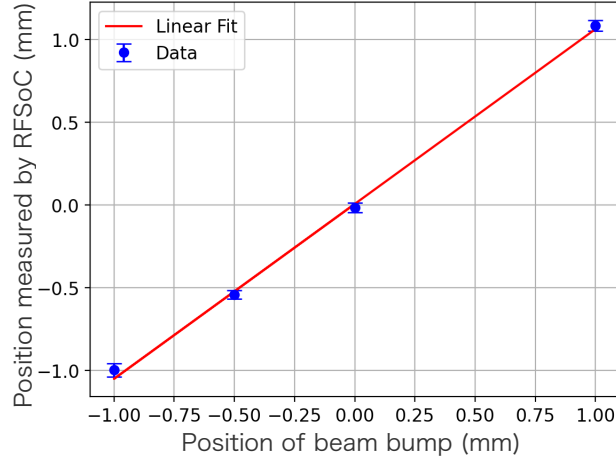


**Figure 11.** Measurement results of the test using a local beam bump. The horizontal axis is the position of the beam bump, and the vertical axis is the vertical beam position measured by the RFSoc-based BOR. The blue plots is the measured point and the red line is the linear fit of these plots.

and the FB-BPM detector is well calibrated. The bunch positions recorded by this detector have an resolution of about  $1\ \mu\text{m}$  [1], and by comparing them with the bunch positions measured by the RFSoc-based BOR, we confirmed that the RFSoc-based BOR was functioning properly as a bunch-by-bunch detector.

Since the role of the BOR is to observe the oscillation of the bunch position, in this test, bunch-by-bunch beam instability was intentionally induced and was simultaneously measured by the RFSoc-based BOR and the FB-BPM detector. To induce beam instability, we inverted the phase of the feedback kicker by 180 degrees while the beam was stored in the ring, which cause an intentional increase in bunch position oscillations. Since the FB-BPM detector and the RFSoc-based BOR use the button electrodes attached to the same chamber shown in Figure 4, it is expected that the bunch positions they measure will be almost the same. This test was carried out on June 6, 2024 using the LER beam. The number of bunches was 393, the bunch current was about 0.5 mA, and the height of the  $\Sigma$  waveform was about 250 mV. Since the bunch current is almost identical to those of the test using the local beam bump in Section 5.2, the resolution of the RFSoc-based BOR in this test is supposed to be about  $30\ \mu\text{m}$ . The beam instability was induced in the vertical direction, and the vertical bunch position was measured by the FB-BPM detector and the RFSoc-based BOR.

The measurement results are presented in Figure 12. The horizontal axis is time and the vertical axis is the measured vertical bunch position. The blue dots represent the positions measured by the FB-BPM detector and the orange dots represent the positions measured by the RFSoc-based BOR. Each point represents one bunch. The timing to invert the phase of the feedback kicker is received by the FB-BPM detector and RFSoc-based BOR, and this is used as a trigger to record the position, so the timing of the plots of the FB-BPM detector and RFSoc-based BOR in Figure 12 is aligned. From about  $150\ \mu\text{s}$  in Figure 12, it can be seen that the bunch position starts to oscillate due to the phase inversion of the feedback kicker. Comparing the FB-BPM detector and RFSoc-based BOR measurements, we see that the amplitude of the oscillations and the time it takes to increase

are almost the same, confirming that the RFSoc-based BOR works properly as a bunch-by-bunch detector.

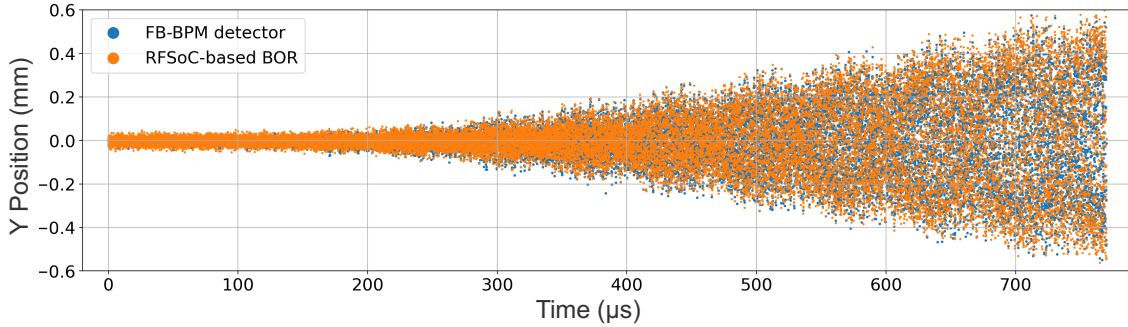


**Figure 12.** Measurement results of the test using feedback system. The blue plots represent the positions measured by the FB-BPM detector and the orange plots represent the positions measured by the RFSoc-based BOR. Each point represents one bunch. Bunch oscillations are increased by inverting the phase of the feedback kicker.

## 6 Observation of Sudden Beam Loss

The RFSoc-based BOR was left connected to the FB-BPM chamber in the Fuji straight section after the tests in Section 5 was completed. SuperKEKB operation resumed at the end of February 2024, and SBL observations using the RFSoc-based BOR were started there.

Figure 13 shows the first SBL event recorded by the RFSoc-based BOR. This is the SBL that occurred at the LER on March 8, 2024. The number of bunches was 783 and bunch current was 0.33 mA. The red dots in the upper half of this figure show the vertical bunch positions, and the blue dots in the lower half show the bunch charges. Each point represents one bunch. The first three turns of the recorded data are used to calculate the average position for each bunch, which is then subtracted from all data as the offset for each bunch. Also, the first three turns of the recorded data are used to calculate the average charge for each bunch, then all the data is divided by this average charge to normalize all bunch charges to 1 when the beam is stable. Figure 13 (left) shows the bunch positions and bunch charges recorded by the RFSoc-based BOR for four turns before the beam abort, with the horizontal axis represents the number of turns before the beam abort. There are two abort gaps of approximately 200 ns each in one turn, so there are two gaps per turn in the plot. Figure 13 (right) is an enlarged view of the dotted-line region in the figure on the left.

Figure 13 (left) shows approximately one turn before the beam is aborted, some bunches are kicked vertically upwards by up to approximately 0.4 mm (dotted-line area). Immediately after that, the bunch charge begin to decrease rapidly, and up to half of the bunch charge was lost. The figure on the right shows that only bunches within a 200 ns width were kicked significantly. Furthermore, the charge of the kicked bunches did not decrease, and it was observed that the charge decrease started from the bunch that came after it. This observation confirmed that when the SBL occurs, the bunches were clearly kicked for an unknown reason, causing oscillations. However, the cause of this kick cannot be determined from these measurements alone.

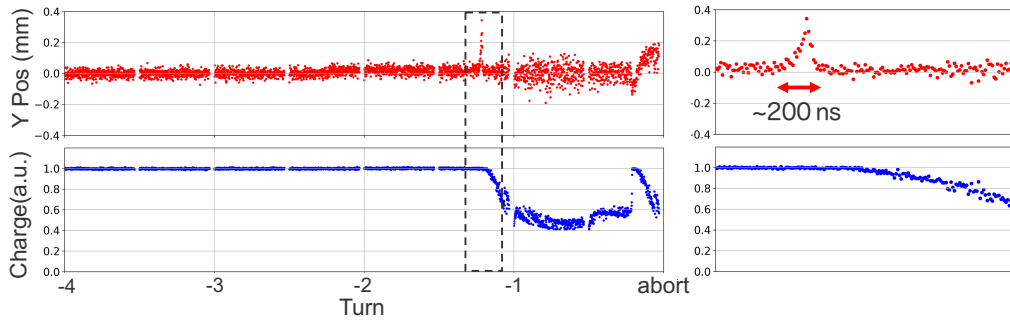


**Figure 13.** The first SBL event recorded with RFSoc-based BOR. This SBL occurred at the LER on March 8, 2024. The number of bunches was 783, and bunch current was 0.33 mA. Left: Vertical position (upper) and charge (bottom) for the last 4 turns before the beam abort. One point corresponds to one bunch. Right: Enlarged view of the dotted line area in the figure on the left.

We continued to record SBLs using the RFSoc-based BOR. Figure 14 shows three examples of the recorded SBLs. The upper plots show the vertical position; and the lower plots show the bunch charge for the last six turns before the beam abort. These plots can be interpreted in the same way as in Figure 13. From the left, 'A' represents an SBL that occurred on March 29, 2024, with 2346 bunches and a bunch current of 0.34 mA. In this event, the bunch position displacement started approximately three turns before the beam abort, and the oscillations seem to get stronger after that. The large charge loss seems to start approximately two turns before the beam abort. 'B' represents an SBL that occurred on April 6, 2024, with 2346 bunches at a bunch current of 0.38 mA. In this event, the bunch position displacement started approximately three turns before the beam abort, and the oscillations seem to get stronger after that. The oscillations are different from those in 'A', and the bunch train seems to be greatly disturbed. The large charge loss seems to start approximately 1.5 turns before the beam abort. 'C' represents an SBL that occurred on April 13, 2024, with 2346 bunches and a bunch current of 0.4 mA. In this event, the bunch position displacement appears to start approximately four turns before the beam abort, and the oscillation begins earlier than in the other examples. However, the amount of charge loss is not as great as in the other examples.

These observational results show that there are various types of bunch position oscillations and charge losses in the SBL. These bunch oscillations are initiated when the bunch receives some kind of kick, but these results indicate the location and strength of the kick vary for each SBL event, and it is still unclear what causes these oscillations. Therefore, it will be difficult to determine the cause of the SBL by looking at only the data from this single BOR. We believe it is important to create more BORs and install them in the SuperKEKB ring to identify the cause of the SBL. It will enable us to cover the betatron phase widely, determine at what betatron phase the bunch oscillations begin, and how the oscillations develop. Furthermore, by using multiple BORs around the area where such a kick is likely to occur, it may be possible to directly narrow down the origin of the SBL. When considering placing many BORs in the ring, the RFSoc-based BOR, which does not require a crate and is easy to carry, is expected to be a very powerful monitor. We plan to create additional RFSoc-based BORs and place them around the entire ring to get closer to identifying the cause of the SBL.

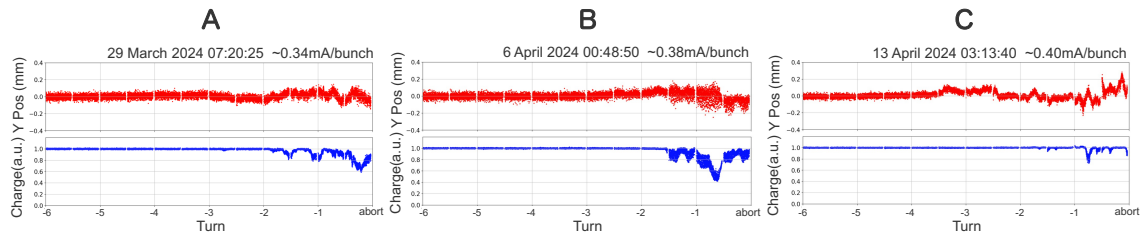


**Figure 14.** Three examples of the SBLs recorded by RFSoc-based BOR. Upper plot shows the vertical position and lower plot shows the bunch charge for the last 6 turns before the beam abort. From left to right, 'A' represents an SBL that occurred on March 29, 2024, with 2346 bunches at a bunch current of 0.34 mA. 'B' represents an SBL that occurred on April 6, 2024, with 2346 bunches at a bunch current of 0.38 mA. 'C' represents an SBL that occurred on April 13, 2024, with 2346 bunches at a bunch current of 0.4 mA.

## 7 Summary

The SuperKEKB accelerator aims to significantly increase luminosity, but a phenomenon known as SBL has emerged as a challenge. This is a phenomenon in which an ampere-class stored beam is suddenly lost in a few turns ( $\sim$ a few tens of  $\mu$ s). SBL can damage accelerator components and Belle II detectors, and quench the superconducting focusing system, which hinders luminosity improvement.

To address and analyze the SBL in detail, we have developed a new BOR based on RFSoc technology. This BOR captures the bunch-by-bunch beam position just before the beam abort occurs. Our RFSoc-based BOR has been verified to function effectively as a bunch-by-bunch monitor, achieving a position resolution of  $30 \mu\text{m}$ . This surpasses the target of  $0.1 \text{ mm}$ . We have initiated SBL observations using the RFSoc-based BOR, successfully recording multiple SBL events.

The data recorded by the RFSoc-based BOR revealed a variety of positional oscillations and charge loss patterns during SBL events. Consequently, we believe that identifying the cause of SBL will require more BORs. In the future, we aim to deploy additional RFSoc-based BORs to cover a wider range of betatron oscillation phases, enabling a more comprehensive investigation of SBL. Furthermore, we intend to use BORs to identify the source of beam instability by strategically positioning them at locations suspected to be the origin of SBL. We anticipate that the newly developed portable, high-speed bunch-by-bunch monitor will bring us closer to resolving SBL.

## 8 Acknowledgements

R. Nomaru and G. Mitsuka work was supported by Japan Society for the Promotion of Science (JSPS) International Leading Research Grant Number JP22K21347. In addition, R. Nomaru work was supported by JSPS Core-to-Core Program (Grant Number: JPJSCCA20230004). L. Ruckman and R. Herbst work was supported by the U.S. Department of Energy, under contract number DE-AC02-76SF00515.

## References

- [1] SuperKEKB Design Report, <https://kds.kek.jp/event/15914/>
- [2] H. Ikeda, T. Abe, M. Aversano, H. Fukuma, Y. Funakoshi, T. Ishibashi, T. Koga, H. Kaji, Y. Liu and G. Mitsuka, *et al.*, “Observation of sudden beam loss in SuperKEKB,” JACoW **IPAC2023**, MOPL072 (2023), doi:10.18429/JACoW-IPAC2023-MOPL072
- [3] T. Ishibashi (private communication, 2024).
- [4] M. Tobiyama and J. W. Flanagan, “Development of Bunch Current and Oscillation Recorder for SuperKEKB Accelerator”, in *Proc. IBIC’12*, Tsukuba, Japan, Oct. 2012, paper MOPA36, pp. 138–142.
- [5] M. Aversano (private communication, 2024).
- [6] "White Paper: An Adaptable Direct RF-Sampling Solution", AMD WP489 (v1.1) February 20, 2019, <https://docs.amd.com/v/u/en-US/wp489-rfsampling-solutions>
- [7] "Technical Overview of AMD RFSoc Technology", AMD Technical Documentation, <https://www.xilinx.com/products/silicon-devices/soc/rfsoc.html>
- [8] AMD Zynq UltraScale+ RFSoc ZCU111 Evaluation Kit, <https://www.xilinx.com/products/boards-and-kits/zcu111.html>
- [9] M. Tobiyama (private communication, 2024).
- [10] M. Tobiyama, H. Fukuma, K. Shibata, M. Tejima, S. Hiramatsu, K. Mori, H. Ishii and T. Obina, “Development of Button Electrodes for SuperKEKB Rings”, Proceedings of BIW10, Santa Fe, New Mexico, US
- [11] Nihon Koshuha Co., Ltd. variable length coaxial tube, [https://www.nikoha.co.jp/coax\\_component/cat01\\_class07/294.html](https://www.nikoha.co.jp/coax_component/cat01_class07/294.html)
- [12] LORCH, <https://www.smithsinterconnect.com/our-company/who-we-are/our-technology-brands/lorch/>
- [13] Keysight Technologies E5071C, <https://www.keysight.com/us/en/product/E5071C/e5071c-ena-vector-network-analyzer.html>
- [14] MACOM H-183-4 datasheet, <https://cdn.macom.com/datasheets/H-183-4.pdf>
- [15] Rohde & Schwarz RTO2000 oscilloscope, [https://www.rohde-schwarz.com/us/products/test-and-measurement/oscilloscopes/rs-rto2000-oscilloscope\\_63493-10790.html](https://www.rohde-schwarz.com/us/products/test-and-measurement/oscilloscopes/rs-rto2000-oscilloscope_63493-10790.html)
- [16] Texas Instruments THS4303EVM, <https://www.ti.com/tool/THS4303EVM>
- [17] Texas Instruments THS4303, <https://www.ti.com/product/THS4303>
- [18] ZCU111 Evaluation Board User Guide (UG1271) - XM500 RFMC Documentation, <https://docs.amd.com/r/en-US/ug1271-zcu111-eval-bd/HW-FMC-XM500>
- [19] Mini-Circuits TCM2-33WX+, <https://www.minicircuits.com/WebStore/dashboard.html?model=TCM2-33WX%2B>
- [20] Anaren BD1631J50100AHF datasheet, [https://www.ttm.com/files/products/wireless-xinger/balun-transformers/BD1631J50100AHF/BD1631J50100AHF\\_DataSheet%28Rev\\_L%29.pdf](https://www.ttm.com/files/products/wireless-xinger/balun-transformers/BD1631J50100AHF/BD1631J50100AHF_DataSheet%28Rev_L%29.pdf)
- [21] AMBA 4 AXI4-Stream Protocol Specification, ARM IHI 0051A (ID030610)
- [22] AMBA AXI and ACE Protocol Specification, ARM ARM IHI 0022E (ID033013)

- [23] Rogue Software Framework, <https://slaclab.github.io/rogue>
- [24] PyDM: a PyQt-based framework for building user interfaces for control systems, <https://slaclab.github.io/pydm>
- [25] M. Tobiyama and J. W. Flanagan, “Bunch by bunch feedback systems for SuperKEKB rings”, Proceedings of the 13th Annual Meeting of Particle Accelerator Society of Japan, August 8-10, 2016, Chiba, Japan, pp. 144-148.
- [26] Dimtel, inc. iGp12, <https://www.dimtel.com/products/igp12>